JJEES

JJEES (2024) 15 (1): 70-76
ISSN 1995-6681

Jordan Journal of Earth and Environmental Sciences

Simulation of Breakthrough Curves of Pb Ions Adsorption by Natural Zeolitic Tuff Using Axial Dispersion and External Mass Transfer Modelsy

Ahmad M. Al-Haj-Ali*[1] and Ali K. Al-Matar[2]

[1]*Prof.*, [2]*Assoc. Prof., Dept. of Chemical Engineering, School of Engineering,* University of Jordan, Amman 11942, Jordan

Received April 12, 2022; Accepted August 27, 2023

Abstract

The axial dispersion model (ADM) was applied to the breakthrough curves data obtained for lead ions removal from aqueous solutions by a natural zeolitic tuff in a lab-scale packed bed column apparatus. The axial dispersion coefficient and Peclet number were determined from simulations at different superficial solution velocities, bed heights, and particle size cuts of the mineral. The axial dispersion coefficient varied from 6.19×10^{-6} to 8.28×10^{-4} $m^2.s^{-1}$ and was found to increase with solution velocity and particle size while decreasing with bed height. The external film mass transfer coefficient was determined for different solution velocities and particle size cuts and was found to be 4.93×10^{-5} to 7.85×10^{-5} $m.s^{-1}$, suggesting a considerable mass transfer resistance.

Keywords: *Adsorption, Zeolitic tuff, Lead ions, Dispersion model, Peclet number, Transfer coefficient.*

1. Introduction

Modeling and simulation are important tools in designing, scaling up, and optimizing environmental engineering processes such as adsorption and ion exchange, which are widely used to remove toxic and objectionable pollutants from water and industrial wastewater (Verma, 2014). In practical industrial-scale systems, these processes are conducted in packed bed columns continuously operated at steady state conditions. Mathematical models formulated to describe a particular process are validated by fitting them to data obtained from laboratory scale experiments and comparing them with the computed output. Physically significant process parameters such as fluid dispersion and mass transfer coefficients are the main targets for evaluation.

Several models have been reported in the literature for packed bed adsorbers. Each model may have a merit over others but suffers drawbacks such as weak correlation, a large number of parameters and unsuitability for multi-stage resistance or multi-component systems. Many research publications on the removal of heavy metal ions, dyestuff, and phenol among chemical pollutants of water focused on the use of empirical kinetic models such as Bohart-Adams, Thomas, Clark and Moon-Nelson (Barrows et al., 2013; Xu et al., 2013). Although these models are useful and simple to use, they give less practical information in terms of mass transfer resistance encountered and the non-ideal behavior of the adsorption system. Models that describe the process's dynamics and mechanism, mostly based on external and/or internal mass transfer resistances and fluid dispersion, have been successfully applied (Inglezakis et. al., 2020; Patel, 2019; Taamneh and Al Dwairi, 2013).

The axial dispersion model (ADM) has been widely used in chemical and environmental process engineering to represent the flow of fluid inside packed bed contactors in combination with models correlating dimensionless groups to express the external film mass transfer effects at the solution/ particle boundaries (Hethnawi et al., 2020; Delgado, 2006). Axial dispersion is the result of coupling molecular diffusion and convection. It is affected by mixing due to splitting and merging flows of liquid around the bed particles. Dispersion and mass transfer coefficients obtained from these models are more useful in packed beds design and operation compared with the empirical kinetic models characterized by pseudo or lump-sum rate constants.

In practical plug-flow column-type reactors, flow is usually non-ideal due to inlet and exit flow disturbances as well as axial dispersion, which is an expression of the degree of back-mixing and deviation from ideal plug flow behavior. Axial dispersion is an important parameter affecting the performance of fixed bed columns (Hill and Root, 2014). The axial dispersion model has been employed for tall columns containing packed beds of porous materials such as cylindrical charcoal particles (Popa et al., 2015).

In this work, the theoretical axial dispersion reactor model has been used to analyze the convective and diffusive mass transfer during Pb ions exchange over Na-saturated zeolitic tuff particles at low fluid velocities. This system is important in environmental applications as natural zeolitic minerals have increasingly demonstrated their efficacy as adsorbents or ion exchange materials for water and wastewater treatment, environmental remediation as well as sub-surface barriers to prevent groundwater pollution (Perez-Botella et al., 2022; Morante-Carballo et al., 2021; Misaelides, 2011). Zeolites are hydrated aluminosilicates

* Corresponding author e-mail: ahmad.ay55@gmail.com

of alkaline and alkaline earth metals that with a unique framework structure associated with remarkable physical and chemical properties. According to Velarde et al., (2023), the properties of natural zeolites include ease of ion exchange, adsorption, dehydration, and rehydration, as well as being eco-friendly, low-cost, regenerative, easily accessible, and available to make them excellent adsorbents.

Zeolitic tuff minerals were generated from the alteration of volcanic tuff located mainly in the northeast and center of Jordan. The Jabal Aritain deposits only contain estimated geological reserves of 170 million tons. Phillipsite, chabazite, and faujasite are the most abundant zeolite minerals found in the Jordanian zeolitic tuff (Nawasreh et al., 2006; Dwairi, 1992). Over the last 25 years, these minerals have been mined, processed, and made commercially available for cement manufacture and agricultural applications.

Environmental applications of Jordanian zeolites, as adsorbents and ion exchangers for pollutant removal, have been the subject of extensive investigation. Published studies from different locations in Jordan over the past three decades have demonstrated that Jordanian zeolite tuffs are efficient adsorbents for the decontamination of industrial effluents containing toxic and radioactive metal ions (Khouri, 2019; Al Dwairi et al., 2013; Taamneh and Al Dwairi, 2013; Al-Shaybe and Khalili, 2009; Ibrahim et al., 2002; Dwairi, 1992).

2. Theory and Mathematical Models

The axial dispersion model is described by Hill and Root (2014) and Fogler (2006) for fixed granular bed contactors receiving one phase fluid flow, dispersed over column length and time. The assumptions of the model are as follows: (1) plug flow at isothermal conditions, (2) homogeneous porosity and size distribution throughout the bed, (3) single component involving no chemical reaction, (4) radial dispersion negligible due to small diameter/ length ratio, and (5) boundary film mass transfer is significant. The model is given by the basic equations below:

$$D_L (\partial^2 C/\partial z^2) - u (\partial C/\partial z) = \partial C/\partial t \quad (1)$$

Initial conditions (at t = 0): $C = C_o$ at $z < 0$ and $C = 0$ at $z > 0$ (2)

Boundary condition at z = 0: $- D_L (\partial C/\partial z) + u (C) = u (C_o)$ at t = 0 and t > 0 (3)

Where > 0 designate the position just inside the column at z = 0. D_L is the axial dispersion coefficient, which is the coefficient that can characterize the degree of back-mixing and quantify the deviation from ideal plug flow behavior.

Exit condition (z = L, t = 0 and t > 0): $dC/dz = 0$ (4)

The solution of this model is simplified by substitution to convert the partial differential equation into an ordinary differential equation:

$$d^2C^*/d\alpha^2 + 2\alpha\, dC^*/d\alpha = 0 \text{ and } \alpha = (z - u.t) /(\sqrt{(4D_L.t)} \quad (5)$$

where: C^* is the dimensionless concentration C/C_o. The boundary conditions become:

$$C^* = 1 \text{ for } \alpha = -\infty \text{ and } C^* = 0 \text{ for } \alpha = \infty \quad (6)$$

For ideal reactors, the mean residence time, $\tau = V/Q = L/u$; since the cross-sectional area is constant. For non-ideal reactors, however, the mean residence time is defined as follows:

$$\tau = {}_0\int^{\infty} t\, E(t)\, dt \quad (7)$$

The solution of the above equations gives C/C_o for different values of $\alpha = f(z, t)$:

$$C/C_o = ½ [1- \text{erf} (1/2 \sqrt{Pe}. (1- t/\tau)/(\sqrt{ t/\tau}))] \quad (8)$$

Where:

$$Pe = u\, d_p/D_L = \text{(rate of bulk fluid convection/rate of adsorbate diffusion)} \quad (9)$$

Pe is the Peclet number for particles, which is used as a direct parameter to measure the relative importance of convective transport (bulk movement of fluid due to its velocity) versus molecular diffusion of adsorbate across the liquid-solid boundary film. High Pe indicates an advective transport dominance, while low Pe indicates a mainly diffuse flow. Pe values around 1.0 indicate comparable significance of the two types of mass transport. A plot of C/C_o versus t/τ gives a breakthrough curve with a shape that is dependent on the values of D_L (or Pe).

The external boundary film mass transfer coefficient, k_f, can be obtained using generalized empirical models or correlations involving the dimensionless groups of Sherwood number (Sh), Reynolds number (Re) and Schmidt number (Sc). The Wilson- Geankoplis (1966) correlation at Reynolds' low number values ($0.0015 < Re < 55$) is commonly used and widely applicable:

$$Sh = (1.09/\epsilon)\, (Re.Sc)^{1/3} \quad (10)$$

Where:

$$Sh = k_f.d_p/D_m ;\ Re = \rho.d_p.u/\mu ;\ Sc = \mu/ \rho.D_m \text{ and } k_f = D_m/\delta \quad (11)$$

D_m is the molecular diffusivity (diffusion coefficient) of metal ions from bulk aqueous solution through a stagnant liquid film with a thickness δ to the external surface of zeolite particle at steady state. It is also noteworthy that Peclet number (Pe) is the product of Re and Sc.

2. Materials and Methods

For the validation of the axial dispersion model suggested in this paper, published breakthrough data on Pb ions removal from aqueous solutions as a single metal by natural zeolite tuff were utilized (Al-Haj-Ali and Al-Hunaidi, 2004). A natural phillipsite zeolitic tuff, from the basaltic desert area of Jabal Aritain in northeastern Jordan, was crushed and sieved into several size fractions using ASTM standard sieve set. XRD showed that the tuff is rich in phillipsite, with calcite as a major impurity (Al-Haj-Ali and Marashdeh, 2014). According to published data reviewed by Khouri (2019), the percentage of phillipsite in Jabal Aritain zeolitic tuff ranges between 27- 49%, with an average of 35%.

Three size fractions (355-500, 500-710, and 710-850 μm) were used. This moderate particle size range, which excludes large particles, is associated with high surface area needed to provide a large number of adsorption sites. Very fine

particles (< 355 µm) are also excluded to avoid blocking fixed bed voidage responsible for creating high operating pressure drop for the liquid passage. Each size fraction was washed with tap water until the dust and fines are removed. The mineral was immersed in 25 $g.dm^{-3}$ solution of pure NaCl in distilled, deionized water at room temperature for 24 h. The solution is replaced by a fresh one, and the mineral continued to be immersed for another 24 h. The Na-treated zeolite was then filtered, washed gently with distilled, deionized water and oven dried at 35°C. Non-sieved zeolitic tuff has a bulk and particle densities of 1035 and 2380 $kg.m^{-3}$, respectively, as well as a surface area of 120 $m^2.g^{-1}$.

The used apparatus consists of bench-mounted glass column, 90 cm in length and 1.5 cm inside diameter (1.767-cm2 cross-sectional area). The column is gently packed with a certain amount NaCl-washed zeolitic tuff to give an appropriate bed height. The feed solution is pumped from a glass storage tank to an overhead constant-level tank made of plexiglass and down flow fed to the column through a glass flow meter. Air bubbles are gently expelled before starting the experiment, and flow control is achieved by valves fitted at the top and at the bottom of the column. Samples from effluent solution are withdrawn at predetermined time intervals and analyzed for metal ion concentrations using a Pye-Unicam atomic absorption spectrophotometer. The bed voidage is 0.40 and is estimated from the ratio of particle diameter to bed diameter as reported by Dixon (1988) and Inglezakis (2010).

Table 1. Lists the experimental conditions at which the considered breakthrough curves were obtained. As evident from the sieving size cuts, all the zeolite particles involved are relatively small (less than 0.85 mm). The column dimensional ratio of 90/1.5 is around 1000 times the mean particle diameter. The adsorption capacity for Pb ions obtained by applying the bed-depth service-time (BDST) analysis was determined to be 24.27, 28.71 and 35.73 $mg.g^{-1}$ for 500-710 µm sieve cut at solution velocities of 36.8, 28.30, and 14.15 $cm.min^{-1}$, respectively (Al-Haj-Ali and Al-Hunaidi, 2004).

4. Results and Discussion

4.1. External Film Mass Transfer

This step is often overlooked as a resistance in the literature on packed-bed dynamic models, although it requires more attention to adequately interpret the process kinetics (Inglezakis et al., 2020). Vilardi et al. (2019) have reported the importance of the mass transfer resistance in their adsorption study of Cr(VI) ions by composite nanomaterials. It was recognized as a rate-controlling factor at the early stages of the breakthrough curves in metal ion removal packed bed systems. This was confirmed to be valid by the application of the Wolborska model to the experimental breakthrough curves of Pb^{2+} ions removal by zeolitic tuff process (Al-Haj-Ali and Al-Hunaidi, 2004). Two important differences appeared upon the application of the Wolborska and ADM model to the experimental breakthrough curves of Pb ions/zeolitic tuff system. Firstly, the Wolborska model was applicable only at the low C/Co range, that is, in the initial stage of the adsorption process, while ADM fitted satisfactorily the whole range of the curves. Secondly, the Wolborska model has one lumped kinetic coefficient which reflects both convective and diffusive mass transfer, whereas the ADM distinguishes between the two transport effects by providing two separate coefficients (the axial dispersion coefficient, $D_{L,}$ and the external film mass transfer coefficient, k_f).

For small particle size range and at low fluid velocities, a focus on external liquid-film mass transfer is justified. In this study, the values of coefficient, k_f, and the liquid-film thickness, δ, were calculated by applying the generalized empirical correlation with appropriate dimensionless groups (equations 10 and 11) to the experimental data. They are presented in Table 2.

Table 1. Summary of Experimental Conditions for Breakthrough Curves.
(Initial Pb ions concentration = 250 mg.dm-3 and temperature of 22ºC).

Solution velocity, u ($cm.min^{-1}$)	Particle size cut, d_p (µm)	Bed height*, L (cm)
14.15 (2.358 x 10^{-3} $m.s^{-1}$)	500-710	4.4
		8.8
		13.2
28.30 (4.717 x 10^{-3} $m.s^{-1}$)	500-710	8.8
	355-500	13.2
	500-710	
	710-850	
	500-710	17.6
36.80 (6.133 x 10^{-3} $m.s^{-1}$)	500-710	13.2
		17.6
		22.0

*Each 4.4 cm bed height is equivalent to 10 g of zeolite.

Table 2. External Film Mass Transfer Properties for Pb Ions at Different Liquid Velocities and Average Zeolite Particle Diameters.

Superficial velocity, u ($m.s^{-1}$)	2.358×10^{-3}	4.717×10^{-3}	6.133×10^{-3}	4.717×10^{-3}	4.717×10^{-3}
Particle size cut*, d_p (μm)	500-710	500-710	500-710	355-500	710-850
Reynolds number, Re	1.574	3.148	4.094	2.226	4.134
Schmidt number, Sc	941.8				
Sherwood number, Sh	31.07	39.15	42.73	34.88	42.87
Mass transfer coefficient, k_f ($m.s^{-1}$)	4.93×10^{-5}	6.21×10^{-5}	6.78×10^{-5}	7.85×10^{-5}	5.19×10^{-5}
Stagnant liquid film thickness, δ (μm)	19.2	15.2	14.0	12.0	18.2
Solution properties:	Density, $\rho = 1000\ kg.m^{-3}$, Dynamic Viscosity, $\mu = 8.9 \times 10^{-4}\ kg.m^{-1}.s^{-1}$ Pb^{2+} Molecular Diffusivity, $D_m = 9.45 \times 10^{-10}\ m^2.s^{-1}$				
Bed voidage, ϵ	0.40				

*Average particle diameter is taken as the geometric mean of upper and lower cut sizes.

The coefficient (k_f) can be directly related to process parameters and solution properties for better illustration of their effects. Deriving a specific correlation from equations 10 and 11 as follows:

$$k_f.d_p/D_m = (1.09/\epsilon)\,(\rho.d_p.u/\mu)^{1/3}\,(\mu/\rho.D_m)^{1/3} \quad (12)$$

$$k_f = (1.09/\epsilon)\,u^{1/3}\,(D_m/d_p)^{2/3} \quad (13)$$

For Pb ions in particular, and using the molecular diffusivity value in Table 2, the correlation becomes:

$$k_f = 2.63 \times 10^{-6}\,u^{1/3}/d_p^{2/3} \quad (14)$$

Equations 13 and14 indicate that k_f increases with superficial solution velocity and decreases with particle size. A perfectly linear plot (correlation coefficient R^2 =1.0) is obtained for k_f versus $u^{1/3}/d_p^{2/3}$ (Figure 1), demonstrating that the Wilson and Geankoplis correlation is appropriate to describe the external mass transfer in this system and process. The calculated increase in kf with temperature increase is 37.5 %, while the decrease in k_f with increasing the average particle diameter is 51%. Another linear correlation (R^2 = 0.99) was obtained by plotting Sherwood number versus Reynolds number as shown in Figure 2. This highlights the importance of external mass transfer resistance in process dynamics under the investigated conditions.

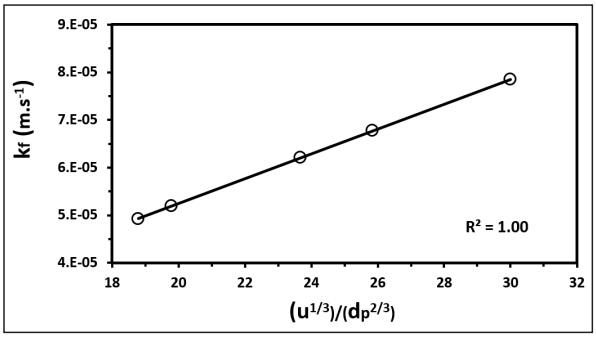

Figure 1. Effect of superficial solution velocity and zeolite particle size on the external film mass transfer coefficient for Pb2+ ions.

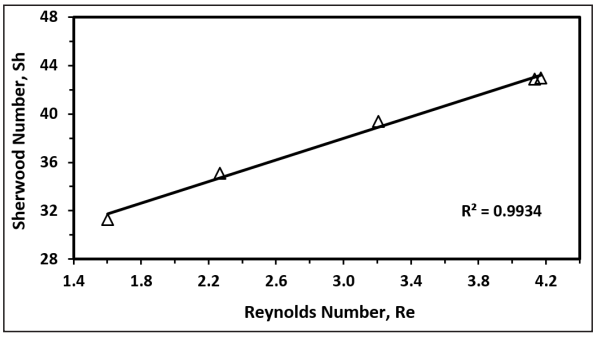

Figure 2. Dependence of Sherwood number on Reynolds number for external film mass transfer.

Table 3. Axial Dispersion Coefficients and Peclet Number Values Calculated by Fitting ADM to Breakthrough Data of Pb /Zeolite System.

Size Cut*, d_p (μm)	u ($m.s^{-1}$)	Re	L (cm)	D_L ($m^2.s^{-1}$)	Pe (-)
500-710	2.358E-03	1.574	4.4	2.935E-05	0.852444
			8.8	1.535E-05	1.704888
			13.2	0.602E-05	2.557333
500-710	4.717E-03	3.148	8.8	4.388E-04	1.704888
			13.2	3.814E-04	2.557333
			17.6	2.385E-04	3.409777
500-710	6.133E-03	4.094	13.2	8.282E-04	2.557333
			17.6	7.057E-04	3.409777
			22.0	6.891E-04	4.262221
355-500	4.717E-03	2.226	13.2	2.1407E-04	3.616614
710-850		4.105		5.529E-04	1.961385

*Average particle diameter is taken as the geometric mean of upper and lower cut sizes.

Moreover, Table 2 reveals that for a given particle size cut (500-710 μm), which is used for most experiments, the stagnant liquid film thickness (δ) decreased from 19.2 to 14.0 μm as solution velocity increased from 14.15 to 36.8 $cm.min^{-1}$. This decrease reveals that external film mass transfer resistance is important at lower solution velocities.

4.2. Axial Dispersion

The ADM equations were solved using common spreadsheet. The model application to experimental breakthrough data (C/C_o versus contact time) enabled the determination of the axial dispersion coefficient (D_L), as well as the Peclet number. It was found that D_L (also known as longitudinal diffusion coefficient or effective diffusivity) is a function of operating conditions including liquid velocity, bed height and zeolite particle size (d_p). Initial Pb ions concentration was kept constant at 250 mg.dm^{-3}, and solution temperature at 22°C. Table 3 summarizes the model fitting results.

The predictions of the model are shown along with experimental breakthrough data (C/C_o vs. contact time) in Figures 3- 5, designated as ADM in the legend. It can be observed from Figure 3 (a, b, c) that the model describes quite well the breakthrough data obtained at different bed heights while keeping liquid velocity constant. Bed height is another expression of the quantity or mass of zeolite available for Pb ions removal which ranged from 4.4 cm (10 g) up to 22 cm (50 g). It is a key parameter in the design of fixed-bed columns. Tall beds allow for longer service time before regeneration is needed. Both the data and the simulation results are consistent with the common trend of sigmoidal shape, where curve flattening is due to the widened mass transfer zone as bed height is increased. This is quite evident at the lower solution velocity (Figure 3, a).

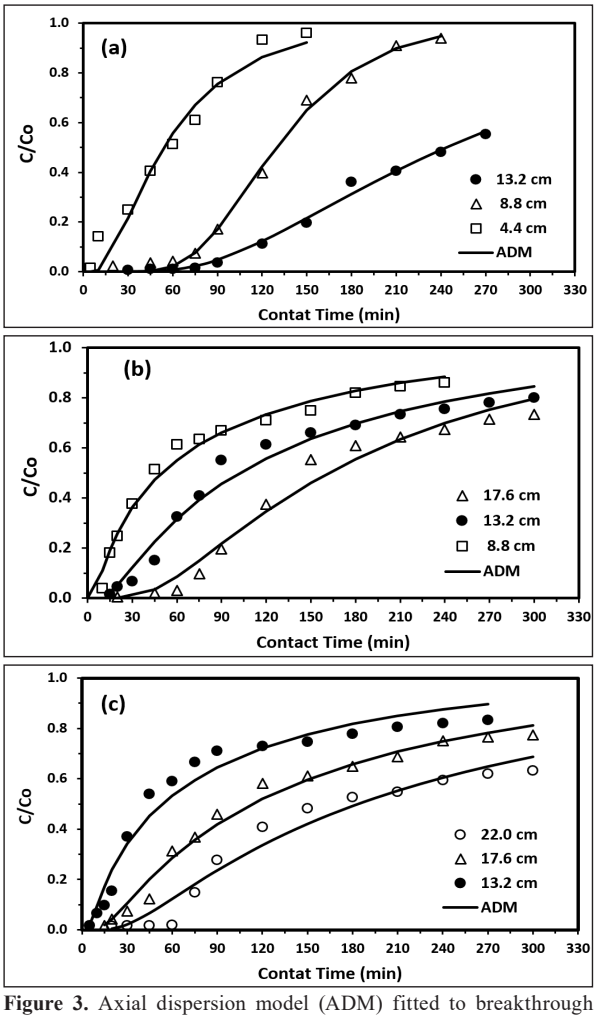

Figure 3. Axial dispersion model (ADM) fitted to breakthrough curves at various bed heights: (a) u = 14.15 cm.min-1 (b) u = 28.3 cm.min-1 (c) u = 36.8 cm.min-1.

The scattering of experimental data around the model representation can be explained in part due to the deviation of actual bed/ column conditions from assumptions on which the model is based, such as the zeolite, which may not be represented accurately in the simulations by the average particle diameter. Taking an average particle diameter instead of full particle size distribution may result in lower values of the axial dispersion coefficients calculated by the model. Also, some of the data scattering and deviation may be attributed to a minor contribution of intraparticle diffusion, which is not usually a part of the mass transfer resistances in the axial dispersion model. Excluding solid diffusion resistance can be justified for using a small particle size range (355-850 µm) and testing a simpler mathematical model.

Figure 4. compares the modeled breakthrough curves plotted at different superficial solution velocities obtained at constant zeolite bed height. Both the experimental data and the fitted ADM are in agreement with expected results of longer breakpoint time, and, thus, higher degree of zeolite bed utilization as the solution velocity is reduced. This result is because more contact time is available for the transfer process of ions from solution to the surface of zeolite particles over a wide mass transfer zone. The effect of solution velocity on axial dispersion coefficient is illustrated quantitatively below.

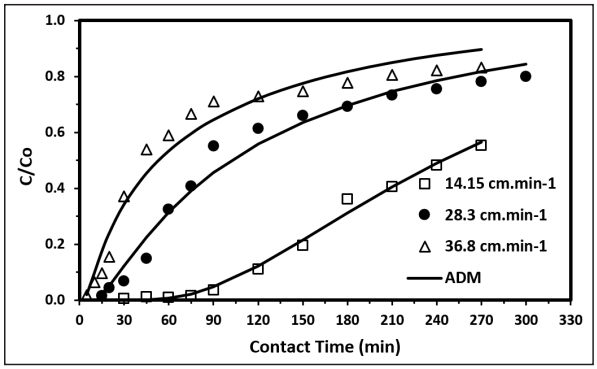

Figure 4. Effect of superficial solution velocity at constant bed height.

The effect of using three zeolite particle size cuts is shown in Figure 5. Compared to the effect of liquid velocity and bed height, the variation in the shape of breakthrough curves or breaktime is not substantial. This variation can be attributed to the relatively narrow size range investigated (355-850 µm or below 0.85mm). Within this size range, it is evident that the lower size cut provided a longer break time and a shape closer to the typical S-curve due to the larger surface area with more ion exchange sites available for Pb^{2+} uptake. A general conclusion from this minor effect of particle size is that intraparticle diffusion is not the main resistance in the process dynamics compared to the effects of fluid dispersion and molecular diffusion.

Effects of superficial solution velocity (u) and zeolite particle size (d_p) on the axial dispersion coefficient are shown in Figure 6 as D_L versus Reynolds number, which is directly proportional to both "u" and "d_p" (equation 11). D_L is strongly dependent on solution velocity where it increased from 6.0 x10^{-6} to 8.2x10^{-4} m^2.s^{-1} when the Reynolds number increased from 1.57 to 4.09 by increasing velocity from 14.15

to 36.8 cm.min^{-1} using the same size cut. For small values of the liquid phase velocity, the increase of the axial dispersion coefficient D_L is negligible, which is in agreement with the findings of Popa et al. (2015) who also reported a dependence of D_L on solution velocity for NaCl tracer solution dispersed through charcoal beds. Similarly, D_L increased by 158% when the particle size cut was changed from 355-500 to 710-850 μm at constant solution velocity. This increase is in agreement with the reported results of studies on similar systems reviewed by Delgado (2006), where the axial dispersion coefficient increased by a factor of 1.5 as the ratio of particle diameters went from a value of 2 to 5.

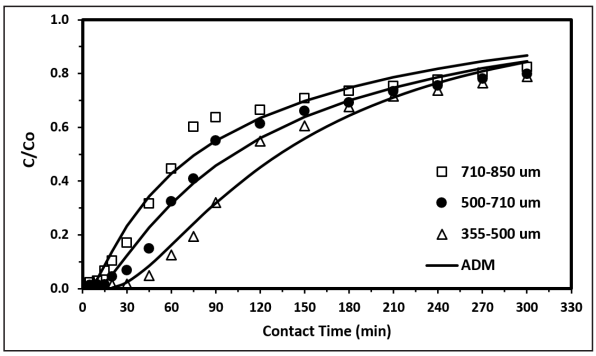

Figure 5. Breakthrough curves using different zeolite particle size cuts.

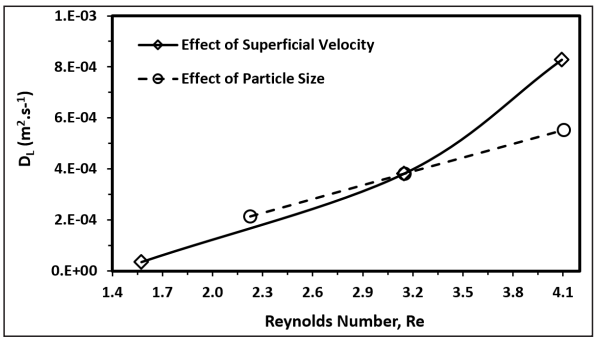

Figure 6. Effects of superficial solution velocity and zeolite particle size on the axial dispersion coefficient.

The effect of bed height on the axial dispersion coefficient is shown in Figure 7 at each of the three studied solution velocities. At 14.15 cm.min^{-1}, D_L is quite low and rather independent of bed height. At a constant bed height of 13.2 cm, D_L is higher with higher velocity. Moreover, at a constant velocity of 28.3 and 36.8 cm.min^{-1}, D_L decreased by 45 and 17 % respectively. Compared with the breakthrough curves shown in Figure 3 (a, b, c), the favorable S-shaped curves are shown to be connected with lower dispersion coefficients (higher Peclet numbers), indicating the dominance of convective (bulk fluid) transport. Similar results were obtained by Yun et al. (2005) who identified a trend of decreasing the axial dispersion (film diffusion) coefficient with increasing bed height, giving more importance to convective transport.

The above observation can be explained on the basis of the Peclet number definition and values (discussed earlier in the theory and model development). Since Pe values are higher than 1.0 for most of the operating conditions (as shown in Table 3), convective (bulk liquid) transport appears to be dominant and thus controls the overall process dynamics. In this case, the values of the dispersion coefficient, D_L, are correspondingly low, indicating negligible diffusion resistance to adsorbate transfer from solution to adsorbent surface. The above inference agrees with the theory and also with studies reported in the literature (Delgado, 2006) that convective transport becomes dominant over molecular diffusion as the fluid flow rate is increased.

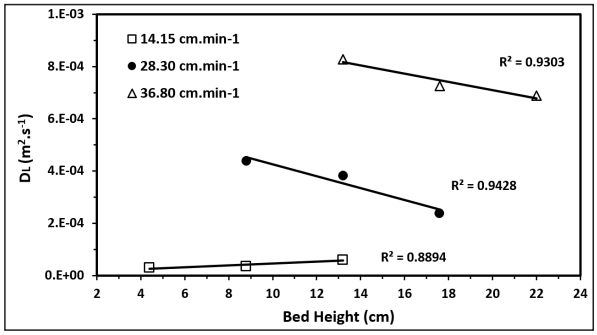

Figure 7. Effect of zeolite bed height on the axial dispersion coefficient of Pb ions.

5. Conclusion

The axial dispersion model is capable of predicting the performance of Pb ions sorption by packed beds of natural zeolite as it was successfully validated with breakthrough curves over variable experimental conditions. The Wilson-Geankoplis correlation describes the external film mass transfer process properly with high correlation coefficient. Both axial dispersion and external film mass transfer coefficients are determined and found to be the functions of the superficial solution velocity and zeolite particle size. D_L is proportional to "u.d_p", whereas k_f is proportional to "u/d_p". Furthermore, D_L decreases with bed height at a given solution velocity.

Small values of both k_f (in the 10^{-5} m.s^{-1} range) and D_L (in the 10^{-4} m.s^{-2} range) indicate that the two mechanisms are significantly important in modeling and describing the considered packed bed system. Axial dispersion is more effective with high liquid velocity, whereas film mass transfer resistance is essential at low flow rates. Both transport effects should be included in analyzing, modeling, and design of metal ions/zeolite adsorption systems.

The model was able to well predict the breakthrough curves of metal ions over the whole contact period, and to provide quantitative information on the effect of mass (metal ion) transfer on the adsorption process dynamics. The above conclusions indicate that using ADM is justified and beneficial to extract the dispersion coefficient (which is the most significant parameter in process dynamics) and mass transfer coefficient from experimental breakthrough data. The ADM would be a means of prediction, scale-up, equipment design, and optimization for the adsorption process.

Nomenclature

ADM: Axial dispersion model

C: Pb ion concentration in solution at any time during the process, mg.dm^{-3}

D_m: Molecular diffusivity of metal ion transferring across stagnant liquid film of thickness δ to the external surface of

zeolite particle, $m^2.s^{-1}$

D_L: Axial dispersion (longitudinal diffusion) coefficient, $m^2.s^{-1}$

d_p: Average diameter of zeolite particle size cut, μm or m

δ: Stagnant liquid-film thickness, μm or m

k_f: External film mass transfer coefficient over liquid-particle interface, $m.s^{-1}$

L: Fixed-bed length, cm

μ: Dynamic viscosity of solution, $kg.m^{-1}.s^{-1}$

ρ: Solution density, $kg.m^{-3}$

t: Contact time, min or s

u: Superficial velocity of solution through the bed, $cm.min^{-1}$ or $m.s^{-1}$

τ: Mean residence time, s

Dimensionless groups:

These are four the packed particles in the bed, where the characteristic length is the average particle diameter, d_p. They are defined in equations 9 and 11:

Pe: Peclet number

Re: Reynolds number

Sc: Schmidt number

Sh: Sherwood number

References

Al Dwairi, R. A., Ibrahim, K.M. and Khoury, H.N. (2013). Potential Use of Faujasite-Phillipsite and Phillipsite-Chabazite tuff in Purification of Treated Effluent from Domestic Wastewater Treatment Plants. Environmental and Earth Sciences 71: 5071-5078

Al-Haj-Ali, A., Al-Hunaidi, T. (2004). Breakthrough Curves and Column Design Parameters for Sorption of Lead by Natural Zeolite. Environmental Technology 25 (9): 1009-1019.

Al-Haj-Ali, A. and Marashdeh, L. (2014). Removal of Aqueous Chromium (III) Ions Using Jordanian zeolite Tuff in Batch and Fixed Bed Modes. Jordan Journal of Earth and Environmental Sciences 6 (2): 45-51.

Al-Shaybe, M., Khalili, F. (2009). Adsorption of Thorium (IV) and Uranium (VI) by Tulul al- Shabba Zeolitic Tuff, Jordan. Jordan Journal of Earth and Environmental Sciences 2 (1):108-109.

Barrows, M.A.S.D., Arroyo, P.A., Silva, E.A. (2013). General Aspects of Aqueous Sorption Process in Fixed Beds. In: Mass Transfer-Advances in Sustainable Energy and Environment Oriented Numerical Modeling, Chapter 14, Edited by Nakajima, H., Intech. DOI: 10.5772/51954.

Delgado, J.M.P.Q. (2006). A Critical Review of Dispersion in Packed Beds. Heat and Mass Transfer 42: 279-310.

Dixon, A.G. (1988). Correlations for Wall and Particle shape effects on fixed bed bulk voidage. Canadian Journal of Chemical Engineering 66: 705-708.

Dwairi, I. (1992) Jordanian Zeolites: Evaluation for Possible Industrial Application of Natural Aritain Phillipsite Tuffs . Dirasat 18(1): 23–44

Fogler, H. S. (2006). Elements of Chemical Reaction Engineering". 4th Ed., Prentice-Hall, New Jersey.

Hethnawi, A., Khderat, W. , Hashlamoun, K., Kanan, A. , Nassar, N.N. (2020). The effect of axial dispersion of lead removal on the fixed bed of natural zeolite. Chemosphere 252: 126523

Hill, C.G., Root, T.W. (2014). Introduction to Chemical Engineering Kinetics and Reactor Design. 2nd Ed., Wiley, New York.

Khouri, H. (2019). Industrial Rocks and Minerals of Jordan: A Review. Arabian Journal of Geosciences 12: 619.

Inglezakis, V. J., Balsamo, M., Montagnaro, F. (2020). Liquid-solid mass transfer in adsorption systems - An Overlooked Resistance? Industrial and Engineering Chemistry Research 59: 22007-22016.

Inglezakis, V. J. (2010). Ion exchange and adsorption fixed bed operations for wastewater treatment, Part-II: Scale-up and approximate design methods, Journal of Engineering Studies and Research 16 (3): 42-50.

Misaelides, P. (2011). Application of natural zeolites in environmental remediation: A short Review. Microporous and Mesoporous Materials 144:15-18.

Morante-Carballo, F., Montalvan -Burbano, N., Carrion-Mero, P., Jacome-Francis, K. (2021). Worldwide Research Analysis on Natural Zeolites as Environmental Remediation Materials. Sustainability 13: 6378.

Nawasreh, M.K., Yasin, S.M., Zurquiah, N.A. (2006). Mineral Status and Future Opportunity: Zeolitic Tuff. Ministry of Energy and Mineral Resources, Amman, Jordan, pp. 19.

Patel, H. (2019). Fixed-bed Column Adsorption Study: A Comprehensive Review. Applied Water Science 9:45.

Perez-Botella, E., Valencia, S., Rey, F. (2022). Zeolites in Adsorption Processes: State of the Art and Future Prospects. Chemical Reviews 122: 17647-17695.

Popa, M., Mamaliga, I., Petrescu, S., Tudose, E.T.I. (2015). Axial Dispersion Study in Fixed Bed Columns. Revista de Chimie 66 (5): 668-672.

Taamneh, Y., Al Dwairi, R. (2013). The Efficiency of Jordanian Natural Zeolite for Heavy Metals Removal. Applied Water Science 3: 77-84.

Verma, A.K. (2014). Process Modelling and Simulation in Chemical, Biochemical and Environmental Engineering. CRC Press, Boca Raton, pp. 377.

Velarde, L., Nabavi, M.S., Escalera, E., Antti, M.-L., Akhtar, F. (2023). Adsorption of Heavy Metals on Natural Zeolites: A Review. Chemosphere 238: 138508.

Vilardi, G., Rodriguez- Rodriguez, J., Ochando-Pulido, J.M., Di Palma, L., Verdone, N. (2019). Fixed-bed Reactor Scale-up and Modelling for Cr(VI) Removal Using nano Iron-based Coated biomass as Packing Material. Chemical Engineering Journal 361(1): 990-998.

Wilson, E. J., Geankoplis, C. J. (1966). Liquid Mass Transfer at Very Low Reynolds Numbers in Packed Peds. Industrial and Engineering Chemistry Fundamentals 5 (1): 9-14.

Xu, Z., Cai, J.-G., Pan, B.-C. (2013). Mathematically Modeling fixed-bed adsorption in aqueous systems. Journal of Zhejiang University (Science A), 14: 155–176.

Yun, J., Yao, S.-J., Lin, D.-Q. (2005). Variation of the local effective axial dispersion coefficient with bed height in expanded beds. Chemical Engineering Journal 109 (1-3): 123-131.